Molecular Therapy
Oncology
Original Article

Exploring prognostic implications of miRNA signatures and telomere maintenance genes in kidney cancer

Srinivasulu Yerukala Sathipati,[1] Sohyun Jeong,[2] Param Sharma,[3] John Mayer,[4] Rohit Sharma,[5] Shinn-Ying Ho,[6,7,8] and Scott Hebbring[1]

[1]Center for Precision Medicine Research, Marshfield Clinic Research Institute, Marshfield, WI 54449, USA; [2]Massachusetts College of Pharmacy and Health Sciences, Boston, MA 02115, USA; [3]Department of Cardiology, Marshfield Clinic Health System, Marshfield, WI 54449, USA; [4]Office of Research Computing and Analytics, Marshfield Clinic Research Institute, Marshfield, WI 54449, USA; [5]Department of Surgical Oncology, Marshfield Clinic Health System, Marshfield, WI 54449, USA; [6]Institute of Bioinformatics and Systems Biology, National Yang Ming Chiao Tung University, Hsinchu 300, Taiwan; [7]College of Health Sciences, Kaohsiung Medical University, Kaohsiung 807378, Taiwan; [8]Biomedical Engineering, National Yang Ming Chiao Tung University, Hsinchu 300, Taiwan

Kidney cancer, particularly clear cell renal cell carcinoma (KIRC), presents significant challenges in disease-specific survival. This study investigates the prognostic potential of microRNAs (miRNAs) in kidney cancers, including KIRC and kidney papillary cell carcinoma (KIRP), focusing on their interplay with telomere maintenance genes. Utilizing data from The Cancer Genome Atlas, miRNA expression profiles of 166 KIRC and 168 KIRP patients were analyzed. An evolutionary learning-based kidney survival estimator identified robust miRNA signatures predictive of 5-year survival for both cancer types. For KIRC, a 37-miRNA signature showed a correlation coefficient (R) of 0.82 and mean absolute error (MAE) of 0.65 years. Similarly, for KIRP, a 23-miRNA signature exhibited an R of 0.82 and MAE of 0.64 years, demonstrating comparable predictive accuracy. These signatures also displayed diagnostic potential with receiver operating characteristic curve values between 0.70 and 0.94. Bioinformatics analysis revealed targeting of key telomere-associated genes such as *TERT*, *DKC1*, *CTC1*, and *RTEL1* by these miRNAs, implicating crucial pathways such as cellular senescence and proteoglycans in cancer. This study highlights the significant link between miRNAs and telomere genes in kidney cancer survival, offering insights for therapeutic targets and improved prognostic markers.

INTRODUCTION

Kidney cancer is among the 10 most common cancers in the United States.[1] Renal cell carcinoma (RCC) accounts for 90% of all kidney cancers.[2] Kidney cancer incidence increases steadily with age, with a worldwide median age at diagnosis of approximately 75 years.[3] The incidence of kidney cancer is approximately 2-fold higher for men than for women, a pattern that appears stable over time and across countries and age groups.[4,5] Hypertension, obesity, and smoking are the well-established risk factors of kidney cancer.[6] Histologically, RCC accounts for the majority (90%) of kidney cancer cases, predominantly including clear cell renal cell carcinoma (KIRC) (70%), papillary RCC (KIRP) (10%–15%), and chromophobe RCC (5%).[7] Disease-specific survival is worst with clear KIRC, as it tends to be diagnosed at a more advanced stage.[8] More than 50% of patients with KIRC are asymptomatic and diagnosed incidentally during thoracoabdominal imaging ordered for unrelated issues.[8,9] As symptoms are often absent in the early stages of the disease, RCC is often only detected once it has already reached an advanced stage.

MicroRNAs (miRNAs) are small (20–24 nucleotides), non-coding, single-stranded RNA molecules that regulate gene expression at the post-transcriptional level. Their main action consists of suppressing gene expression by recognizing the complementary 3′ untranslated region (UTR) of the target mRNA, leading to its cleavage with subsequent degradation or translation inhibition.[10] It is estimated that about 30% of human genes are regulated by miRNAs,[11] making them significant in many basic biological processes including development, cell differentiation, proliferation, and apoptosis. Dysregulation of miRNA expression plays a role in the pathogenesis of many diseases including cancers; the impact of altered miRNA expression has been well documented in many types of cancer. miRNAs have also been proposed as useful diagnostic biomarkers for cancers.[12] Evidence has emerged supporting the utility of miRNAs as predictive biomarkers in kidney cancers.[13] Gottardo et al. identified four up-regulated miRNAs—hsa-miR-28, hsa-miR-185, hsa-miR-27, and hsa-let-7f-2—compared with healthy kidney tissue.[14] Huang et al. reported three differentially expressed miRNAs (hsa-miR-21-5p, hsa-miR-223-3p, and hsa-miR-365a-3p) that can serve as prognostic indicators in patients with KIRC.[15] Additionally, Ng and Taguchi employed a tensor

Received 6 May 2024; accepted 5 September 2024;
https://doi.org/10.1016/j.omton.2024.200874.

Correspondence: Srinivasulu Yerukala Sathipati, Center for Precision Medicine Research, Marshfield Clinic Research Institute, Marshfield, WI 54449, USA.
E-mail: sathipathi.srinivasulu@marshfieldclinic.org
Correspondence: Scott Hebbring, Center for Precision Medicine Research, Marshfield Clinic Research Institute, Marshfield, WI 54449, USA.
E-mail: hebbring.scott@marshfieldresearch.org

decomposition-based unsupervised feature extraction method to analyze mRNA and miRNA expression profiles in KIRC, identifying 23 genes significantly correlated with patient survival.[16]

Telomeres are repetitive DNA elements at the ends of chromosomes necessary to maintain chromosomal stability. In most cell types, telomeres shorten with each cell division. An accumulation of critically short telomeres induces cellular senescence and apoptosis, mechanisms generally inactive in cancer cells. MicroRNAs (miRNAs) have been implicated in controlling telomere function in cancerous cells.[17–19] For example, telomerase reverse transcriptase (*TERT*) is implicated in the regulation of miRNAs by modulating their genesis. Decreased *TERT* levels are linked to lower primary miRNA production, influencing both telomere length and the progression of cancer.[20–22] Moreover, 12.2% of KIRC cases have somatic mutations in *TERT*, suggesting a unique pathogenesis and aggressive disease trajectory.[23] Despite the recognized importance of miRNAs and telomere maintenance (TM) genes in kidney cancers, their interrelationship remains under-investigated. Understanding this connection could enhance the knowledge of kidney cancer mechanisms and aid in developing more effective treatments.

To identify a prognostic miRNA signature capable of predicting survival time in individuals with kidney cancers, we developed the Kidney cancer Survival Estimation (KSE) method. KSE is a fusion of KIRC survival and KIRP survival methodologies. The core methodology of KSE involves integrating support vector regression (SVR) and an optimal feature selection algorithm. Through this approach, KSE identified miRNA signatures capable of estimating survival times in both KIRC and KIRP. Subsequently, our investigation explored miRNA signatures and TM genes in the context of kidney cancers. An overview of the study is presented in Figure 1.

RESULTS

miRNA signature selection

We employed the kidney cancer survival estimation (KSE) method to assess the survival times of patients diagnosed with KIRC and KIRP. The integration of both models was referred to as KSE. To ensure the reliability of miRNA signatures, we conducted 50 independent runs for both KSE-clear cell renal cell carcinoma (KSE-RC) and KSE-renal papillary cell carcinoma (KSE-RP), aiming to derive a robust feature set and estimation model.

For KSE-RC, the highest estimation performance model selected 37 miRNAs as a signature, yielding a correlation coefficient (R) and mean absolute error (MAE) of 0.84 and 0.64 years between actual and estimated survival times. The KSE-RC-Mean, averaging 32 features, resulted in a mean R and MAE of 0.82 ± 0.01 and 0.65 ± 0.01 years, respectively. Notably, a robust miRNA signature was identified during the 31st independent run (refer to Figure S1A). The KSE-RC-Robust model, featuring 37 miRNAs, achieved an R and MAE of 0.81 and 0.65 years, respectively. The estimation performance of KSE-RC is shown in Table 1. The correlation plot for KSE-RC is shown in Figure S1B.

Similarly, for KSE-RP, the highest estimation performance model selected 23 miRNAs as a signature, showing an R and MAE of 0.83 and 0.61 years, respectively, in the comparison of actual and estimated survival times. Employing the KSE-RP-Mean, which selected an average of 32 features, resulted in a mean R and MAE of 0.80 ± 0.01 and 0.66 ± 0.03 years, respectively. A robust miRNA signature was selected during the 40th independent run (refer to Figure S2A). The KSE-RP-Robust model achieved an R and MAE of 0.82 and 0.64 years, respectively, when comparing actual and estimated survival times. The estimation performance of KSE-RP is shown in Table S1. The correlation plot for KSE-RP is shown in Figure S2B.

Comparative analysis of predictive models

We evaluated the predictive performance of the KSE method against various established machine learning techniques, including linear regression, sequential minimal optimization (SMO) regression, least absolute shrinkage and selection operator (LASSO), and elastic net. For KIRC, KSE-RC showed superior performance over linear regression, SMO, Ridge, and LASSO in terms of R and MAE. KSE achieved an R ranging from 0.42 to 0.82 and an MAE between 0.68 and 1.12 years. KSE's performance was on par with elastic net, yielding an R of 0.84 and an MAE of 0.64 years, using only 39 miRNAs compared with elastic net's 72 miRNAs. The detailed performance metrics are presented in Table 1.

In the case of KIRP, KSE-RP outperformed standard machine learning methods like linear regression, SMO, Ridge, LASSO, and elastic net in terms of R and MAE. The KSE-RP model for KIRP, incorporating 23 miRNAs, achieved an R of 0.82 and an MAE of 0.64 years, surpassing other methods that ranged from 0.39 to 0.65 in R and 0.98 to 1.08 years in MAE. The detailed performance metrics are presented in Table S1.

miRNA signatures in KIRC and KIRP

Utilizing the miRNA frequency (mi*Rf*) score method, we identified distinct miRNA signatures for KIRC and KIRP. For KIRC, the KIRC-mi*Rf* model revealed a 37-miRNA signature, while the KIRP-mi*Rf* model identified a 23-miRNA signature for KIRP. Main effect difference (MED) analysis[24] was then applied to prioritize miRNAs within these signatures. MED analysis can be interpreted such that a higher MED score represents a larger contribution of that miRNA to survival estimation, while a lower score indicates a smaller contribution.

In KIRC, the top 10 miRNAs were hsa-miR-26a-1-3p, hsa-miR-28-5p, hsa-miR-3913-5p, hsa-miR-3170, hsa-miR-148a-5p, hsa-miR-671-3p, hsa-miR-224-3p, hsa-miR-10a-5p, hsa-miR-29b-1-5p, and hsa-miR-106b-5p (shown in Table 2).

For KIRP, the leading miRNAs were hsa-miR-450b-5p, hsa-miR-590-5p, hsa-miR-376c-3p, hsa-miR-500a-5p, hsa-miR-18a-3p, hsa-miR-362-5p, hsa-miR-455-5p, hsa-miR-452-5p, hsa-miR-3928-3p, and hsa-miR-214-5p. Interestingly, only hsa-miR-214-5p was common between the two cancer types, highlighting the distinct nature of each miRNA signature (shown in Table S2).

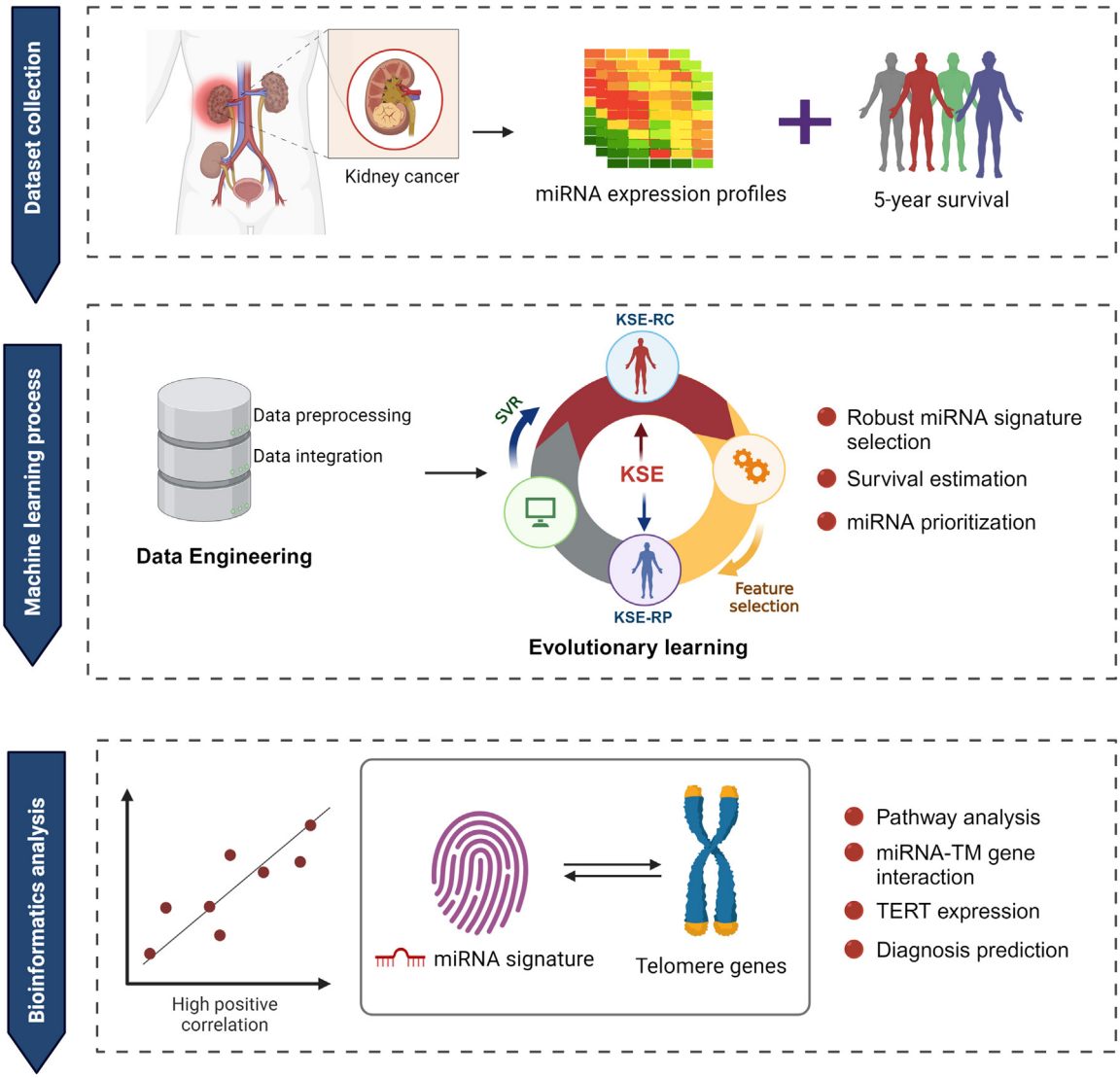

Figure 1. Overview of the study

MiRNA expression profiles of kidney cancer patients, encompassing KIRC and KIRP, were extracted alongside their respective survival times. The machine learning process involved data engineering, the implementation of an evolutionary learning method, robust feature set selection, survival estimation, and miRNA prioritization. Bioinformatics analysis was conducted on the identified miRNA signature and telomere maintenance genes to elucidate their roles in kidney cancers. This figure was created with BioRender.com.

Expression analysis of miRNA signatures in cancer vs. healthy samples

Differential expression of miRNA signatures was analyzed in KIRC and KIRP compared with healthy samples. For KIRC, 69 healthy samples were included, and for KIRP, 34 healthy samples. In the KIRC signature, seven out of the top 10 miRNAs (hsa-miR-26a-3p, hsa-miR-28-5p, hsa-miR-3170, hsa-miR-148a-5p, hsa-miR-224-3p, hsa-miR-10a-5p, and hsa-miR-106b-5p) showed significant expression differences ($p < 0.05$) between cancerous and healthy tissues, as reported in Table 3.

In the KIRP signature, eight out of the top 10 miRNAs (hsa-miR-450b-5p, hsa-miR-590-5p, hsa-miR-376c-3p, hsa-miR-500a, hsa-miR-18a, hsa-miR-362-5p, hsa-miR-455-5p, and hsa-miR-214-5p) demonstrated significant differential expression ($p < 0.05$), as shown in Table S3.

Diagnostic predictive power of miRNA signatures

In KIRC, receiver operating characteristic (ROC) analysis identified 11 miRNAs with high prognostic potential (ROC >0.80), including

Table 1. Estimation performance of KSE-RC

Method	R	MAE (months)	Selected features
Linear regression	0.42	13.44	37
SMO regression	0.43	13.55	37
Ridge	0.8	10.03	422
LASSO	0.82	8.75	25
Elastic net	0.84	8.2	72
KSE-RC	0.84	7.68	37

R, correlation coefficient; MAE, mean absolute error.

hsa-miR-106b-5p, hsa-miR-25-3p, and hsa-miR-10a-5p, among others. These miRNAs had ROC values ranging from 0.95 to 0.81 (Table 3). Specifically, six miRNAs (hsa-miR-106b-5p, hsa-miR-10a-5p, hsa-miR-26a-1-3p, hsa-miR-28-5p, hsa-miR-3170, and hsa-miR-224-3p) were identified as strong prognostic predictors (ROC >0.70), depicted in Figure 2.

For the KIRP signature, seven miRNAs emerged as top diagnostic predictors (ROC >0.80), including hsa-miR-214-5p, hsa-miR-675-3p, and hsa-miR-376c-3p, with ROC values between 0.94 and 0.83 (Table S3). Among the top 10 miRNAs, five (hsa-miR-214-5p, hsa-miR-376c-3p, hsa-miR-362-5p, hsa-miR-500a-5p, and hsa-miR-455-5p) demonstrated strong diagnostic potential (ROC >0.70), with ROC values from 0.94 to 0.77, illustrated in Figure S3.

MiRNA-mutation association

We employed an integrative approach to examine the relationship between miRNA expression levels and genetic mutations in both KIRC and KIRP. The analysis involved preprocessing miRNA and mutation datasets, ensuring alignment by patient identifiers. For KIRP, we focused on the top 10 miRNAs, including hsa-miR-450b-5p, hsa-miR-590-5p, hsa-miR-376c-3p, hsa-miR-500a-5p, hsa-miR-18a-3p, hsa-miR-362-5p, hsa-miR-455-5p, hsa-miR-452-5p, hsa-miR-3928-3p, and hsa-miR-214-5p. For KIRC, we analyzed hsa-miR-26a-1-3p, hsa-miR-28-5p, hsa-miR-3913-5p, hsa-miR-3170, hsa-miR-148a-5p, hsa-miR-671-3p, hsa-miR-224-3p, hsa-miR-10a-5p, hsa-miR-29b-1-5p, and hsa-miR-106b-5p.

The miRNA expression data were transformed into a long format for ease of analysis, and mutation data were filtered for common genes associated with KIRC and KIRP, such as VHL, TP53, TSC1, and PBRM1. Merging the miRNA expression data with mutation data, we grouped by patient ID and gene symbols to summarize miRNA expression and mutation status. MiRNA expression levels were categorized into occurrence levels (high, moderate, and low) and linked to specific genetic mutations. Our findings reveal distinct patterns of miRNA expression correlated with genetic alterations in both KIRC and KIRP. The detailed summary tables generated from this analysis are provided in Tables S4 and S5. The top 10 ranked miRNAs in both KIRC and KIRP, and their mutation correlation are depicted in Figure 3 (for KIRC), and Figure S4 (for KIRP).

Table 2. Individual contribution of miRNAs in KIRC survival estimation

Rank	miRNA	MIMAT ID	MED
1	hsa-miR-26a-1-3p	MIMAT0004499	1.359359
2	hsa-miR-28-5p	MIMAT0000085	1.32198
3	hsa-miR-3913-5p	MIMAT0018187	1.272719
4	hsa-miR-3170	MIMAT0015045	1.206988
5	hsa-miR-148a-5p	MIMAT0004549	1.204212
6	hsa-miR-671-3p	MIMAT0004819	0.885195
7	hsa-miR-224-3p	MIMAT0009198	0.868676
8	hsa-miR-10a-5p	MIMAT0000253	0.837751
9	hsa-miR-29b-1-5p	MIMAT0004514	0.749882
10	hsa-miR-106b-5p	MIMAT0000680	0.745949
11	hsa-miR-1270	MIMAT0005924	0.708113
12	hsa-miR-191-3p	MIMAT0001618	0.695488
13	hsa-miR-214-5p	MIMAT0004564	0.665915
14	hsa-miR-192-3p	MIMAT0004543	0.653562
15	hsa-miR-26a-2-3p	MIMAT0004681	0.520749
16	hsa-miR-185-5p	MIMAT0000455	0.511302
17	hsa-miR-339-5p	MIMAT0000764	0.498169
18	hsa-miR-625-5p	MIMAT0003294	0.484835
19	hsa-miR-582-5p	MIMAT0003247	0.480073
20	hsa-miR-139-3p	MIMAT0004552	0.473633
21	hsa-miR-125b-2-3p	MIMAT0004603	0.432174
22	hsa-miR-150-3p	MIMAT0004610	0.415235
23	hsa-miR-23b-5p	MIMAT0004587	0.404089
24	hsa-miR-152-3p	MIMAT0000438	0.40352
25	hsa-miR-146a-5p	MIMAT0000449	0.398423
26	hsa-miR-205-5p	MIMAT0000266	0.377166
27	hsa-miR-628-3p	MIMAT0003297	0.322882
28	hsa-miR-365a-3p	MIMAT0000710	0.313084
29	hsa-miR-1271-5p	MIMAT0005796	0.297337
30	hsa-miR-769-3p	MIMAT0003887	0.220694
31	hsa-miR-17-3p	MIMAT0000071	0.19183
32	hsa-miR-25-3p	MIMAT0000081	0.179736
33	hsa-miR-136-5p	MIMAT0000448	0.175167
34	hsa-miR-33a-3p	MIMAT0004506	0.166947
35	hsa-miR-154-5p	MIMAT0000452	0.14867
36	hsa-miR-487b-3p	MIMAT0003180	0.145981
37	hsa-miR-425-5p	MIMAT0003393	0.096971

MED, main effect difference.

MiRNAs differentially expressed in different cancer stages by limma pairwise comparison

In the dataset, advanced stages of cancer, specifically stage IV, are characterized by the presence of metastasis to other organs. Patients with stage IV cancer in the dataset have documented metastatic disease, indicating that the cancer has spread beyond the primary site to distant organs. This detailed clinical staging information was included

Table 3. KIRC-miRNA signature expression across cancer andhealthy groups and diagnostic prediction

KIRC signature	Cancer vs. healthy (*p* value)	ROC
hsa-miR-26a-1-3p	4.19E−21	0.84
hsa-miR-28-5p	1.24E−12	0.76
hsa-miR-3913-5p	0.91	0.5
hsa-miR-3170	2.52E−11	0.74
hsa-miR-148a-5p	1.02E−05	0.66
hsa-miR-671-3p	1.90E−01	0.55
hsa-miR-224-3p	3.98E−10	0.73
hsa-miR-10a-5p	2.88E−25	0.88
hsa-miR-29b-1-5p	6.70E−01	0.52
hsa-miR-106b-5p	3.57E−35	0.95
hsa-miR-1270	6.35E−18	0.82
hsa-miR-191-3p	1.97E−11	0.74
hsa-miR-214-5p	5.51E−25	0.88
hsa-miR-192-3p	2.10E−02	0.58
hsa-miR-26a-2-3p	7.00E−02	0.57
hsa-miR-185-5p	7.15E−15	0.78
hsa-miR-339-5p	3.30E−01	0.46
hsa-miR-625-5p	7.19E−03	0.6
hsa-miR-582-5p	2.90E−02	0.58
hsa-miR-139-3p	2.00E−15	0.79
hsa-miR-125b-2-3p	1.13E−03	0.62
hsa-miR-150-3p	5.77E−07	0.68
hsa-miR-23b-5p	6.44E−11	0.74
hsa-miR-152-3p	1.30E−01	0.56
hsa-miR-146a-5p	7.07E−17	0.81
hsa-miR-205-5p	5.82E−15	0.78
hsa-miR-628-3p	1.20E−01	0.55
hsa-miR-365a-3p	1.58E−19	0.83
hsa-miR-1271-5p	2.69E−18	0.82
hsa-miR-769-3p	6.00E−02	0.57
hsa-miR-17-3p	1.77E−04	0.64
hsa-miR-25-3p	1.41E−33	0.94
hsa-miR-136-5p	7.28E−24	0.87
hsa-miR-33a-3p	3.77E−06	0.67
hsa-miR-154-5p	3.94E−23	0.86
hsa-miR-487b-3p	1.67E−09	0.72
hsa-miR-425-5p	2.70E−02	0.58

ROC, receiver operating characteristic curve.

alongside each patient's molecular data to provide a comprehensive understanding of the cancer progression in our analyses. By pairwise comparisons, several miRNAs demonstrated significantly different expressions. In KIRC, hsa-miR-214-5p and hsa-miR-26a-2-3p showed increased expression in stage II compared with stage I, whereas decreased expression in stage IV compared with stage II. Hsa-miR-625-5p and hsa-miR-425-5p were decreased in stage IV compared with stage III. Hsa-miR-139-3p showed increased trend in all advanced stages of cancer. On the contrary, hsa-miR-625-5p showed a decreased trend in all advanced stages of cancer (Table S6). In KIRP, hsa-miR-214-5p and hsa-miR-937-3p increased in stage II compared with stage I but showed decreased trend in all other stage comparisons. In stage III vs. stage IV comparison, only hsa-miR-500a-5p was significantly increased (beta: 0.115, *p* value: 0.007) (Table S6).

The limma association results comparing miRNA expression in stage I to later stages revealed three significant miRNAs in KIRC. Hsa-miR-182-5p demonstrated decreased expression in stage IV compared with stage I (coefficient: −0.564, *p* value: 0.043). Hsa-miR-301a-3p and hsa-imR-136-3p showed increased expression in stage III (coefficient: 0.315, *p* value: 0.036) and stage II (coefficient: 0.540, *p* value: 0.040), respectively. Additionally, has-miR-197-3p exhibited significant associations with overall survival (OS), progression-free interval (PFI), and disease-specific survival (DSS) in KIRC, indicating beneficial effects on survival and cancer treatment. However, hsa-miR-182-5p presented inconsistent results, demonstrating a decrease in stage IV compared with stage I but was associated with decreased DSS.

In KIRP, only has-miR-1251-5p showed significant association in stage II (coefficient: 1.157, *p* value: 0.014), indicating increased expression compared with stage I (Table S6). Increased has-miR-125b-2-3p was associated with PFI; however, none of these associations surpassed multiple testing correction (false discovery rate [FDR]).

Analysis of miRNA signatures and their target TM genes

Our investigation focused on the relationship between miRNA signatures and TM genes. We examined the relation between miRNA signature and TM genes using miRNA-gene target prediction. This was conducted through miRNA-gene target prediction analysis. Utilizing the miRTarBase,[25] we identified validated target genes for both KIRC and KIRP-miRNA signatures. The KIRC signature was found to target 138 genes out of 165 validated TM genes. In contrast, the KIRP signature targets a smaller set of eight TM genes, including *ATM, CTC1, SP1, ESR1, BAZ2A, KDM1A, TP53*, and *HOXA7*. Figure 4A illustrates the top 10 miRNAs from the KIRC signature and their corresponding TM gene targets. The TM gene targets associated with the KIRP signature are depicted in Figure 4B.

To define the efficiency of selected miRNAs in targeting TM genes, we employed a computational approach using TargetScan (v7.0).[26] We focused on the top 10 miRNAs identified in our integrative analysis for KIRC and KIRP. For KIRC, these miRNAs included hsa-miR-26a-1-3p, hsa-miR-28-5p, hsa-miR-3913-5p, hsa-miR-3170, hsa-miR-148a-5p, hsa-miR-671-3p, hsa-miR-224-3p, hsa-miR-10a-5p, hsa-miR-29b-1-5p, and hsa-miR-106b-5p. For KIRP, the top miRNAs were hsa-miR-450b-5p, hsa-miR-590-5p, hsa-miR-376c-3p, hsa-miR-500a-5p, hsa-miR-18a-3p, hsa-miR-362-5p, hsa-miR-455-5p, hsa-miR-452-5p, hsa-miR-3928-3p, and hsa-miR-214-5p. Using TargetScan, we obtained the context++ scores and context++ score percentiles for the interactions between these miRNAs and

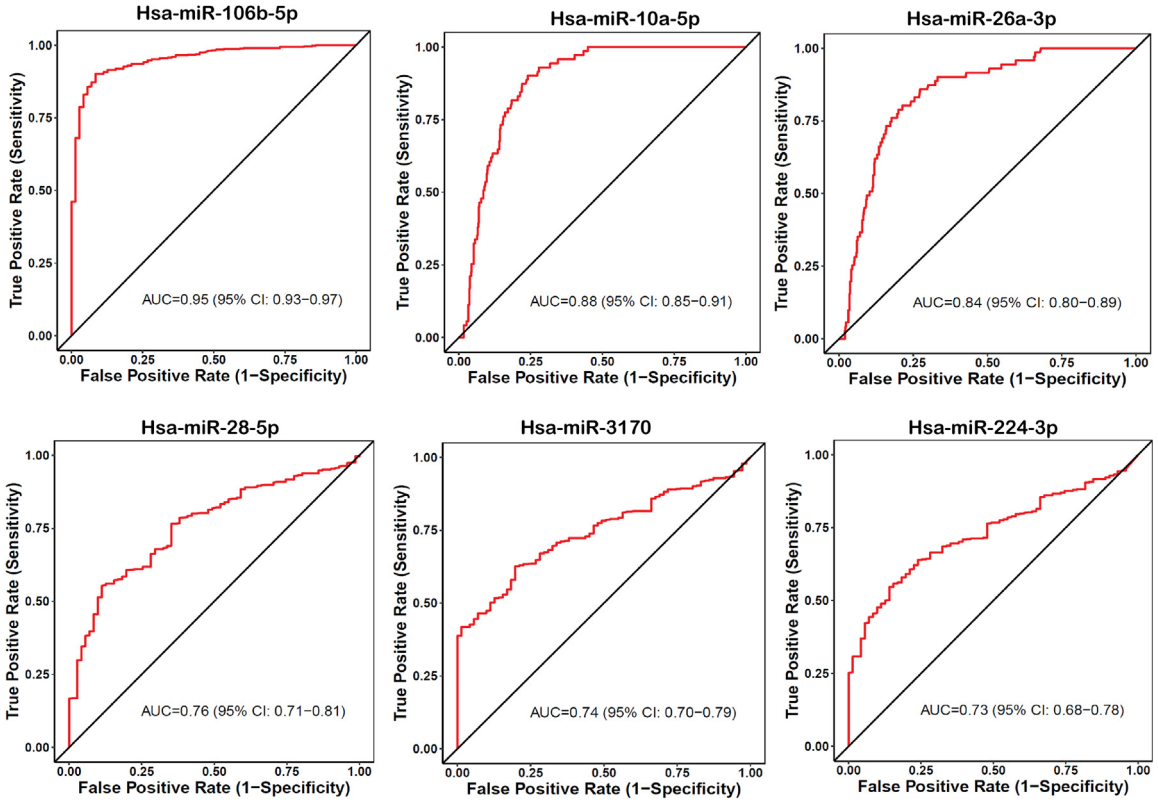

Figure 2. The diagnostic prediction performance of the top ranked KIRC miRNAs was evaluated using ROC curves

TM genes. By applying a stringent context++ score percentile threshold of 70, we identified the most effective miRNA-target interactions. This led us to find that KIRC miRNAs efficiently targeted 29 TM genes, while KIRP miRNAs targeted 27 TM genes. The results of this analysis for KIRC and KIRP miRNAs are provided in Tables S7 and S8, respectively. These findings highlight the potential regulatory roles of these miRNAs in telomere maintenance, providing a basis for further experimental validation.

Biological significance of miRNA signatures in KIRC and KIRP

KEGG pathways

To elucidate the biological relevance of the miRNA signatures identified in KIRC and KIRP, we conducted a pathway analysis using the Kyoto Encyclopedia of Genes and Genomes (KEGG). Utilizing tools such as miRWalk,[27] gene set enrichment analysis,[28] and MIENTURNET,[29] we identified the top 5 significant pathways ($p < 0.05$) in KIRC. These pathways include adherens junction (hsa04520), pancreatic cancer (hsa05212), bladder cancer (hsa05219), proteoglycans in cancer (hsa05205), and epidermal growth factor receptor (EGFR) tyrosine kinase inhibitor resistance (hsa01521). Notably, the renal cell carcinoma pathway (hsa05211) was identified as a key pathway within the KIRC signature.

In the case of KIRP, the analysis highlighted five significant pathways: longevity regulating pathway (hsa04211), endocrine resistance (hsa01522), cellular senescence (hsa04218), FoxO signaling pathway (hsa04068), and p53 signaling pathway (hsa04115). Comprehensive details of these significant KEGG pathways for both KIRC and KIRP are presented in Tables S9 and S10, respectively.

Gene ontology annotations in KIRC and KIRP

Gene ontology (GO) annotations categorize biological entities into three domains: biological processes (BPs), molecular functions (MFs), and cellular components (CCs). In our investigation of both KIRC and KIRP signatures, we applied GO to delineate their functional characteristics.

KIRC signature GO annotations

The prominent BPs for KIRC include positive regulation of protein phosphorylation (GO:0001934), protein phosphorylation (GO:0006468), cellular response to starvation (GO:0009267), negative regulation of gene expression (GO:0010629), and negative regulation of translation (GO:0017148).

Key MFs identified in KIRC encompass protein serine threonine kinase activity (GO:0004674), transforming growth factor beta-activated receptor activity (GO:0005024), histone deacetylase binding (GO:0042826), DNA-binding transcription factor activity (GO:0003700), and GTPase activity (GO:0003924).

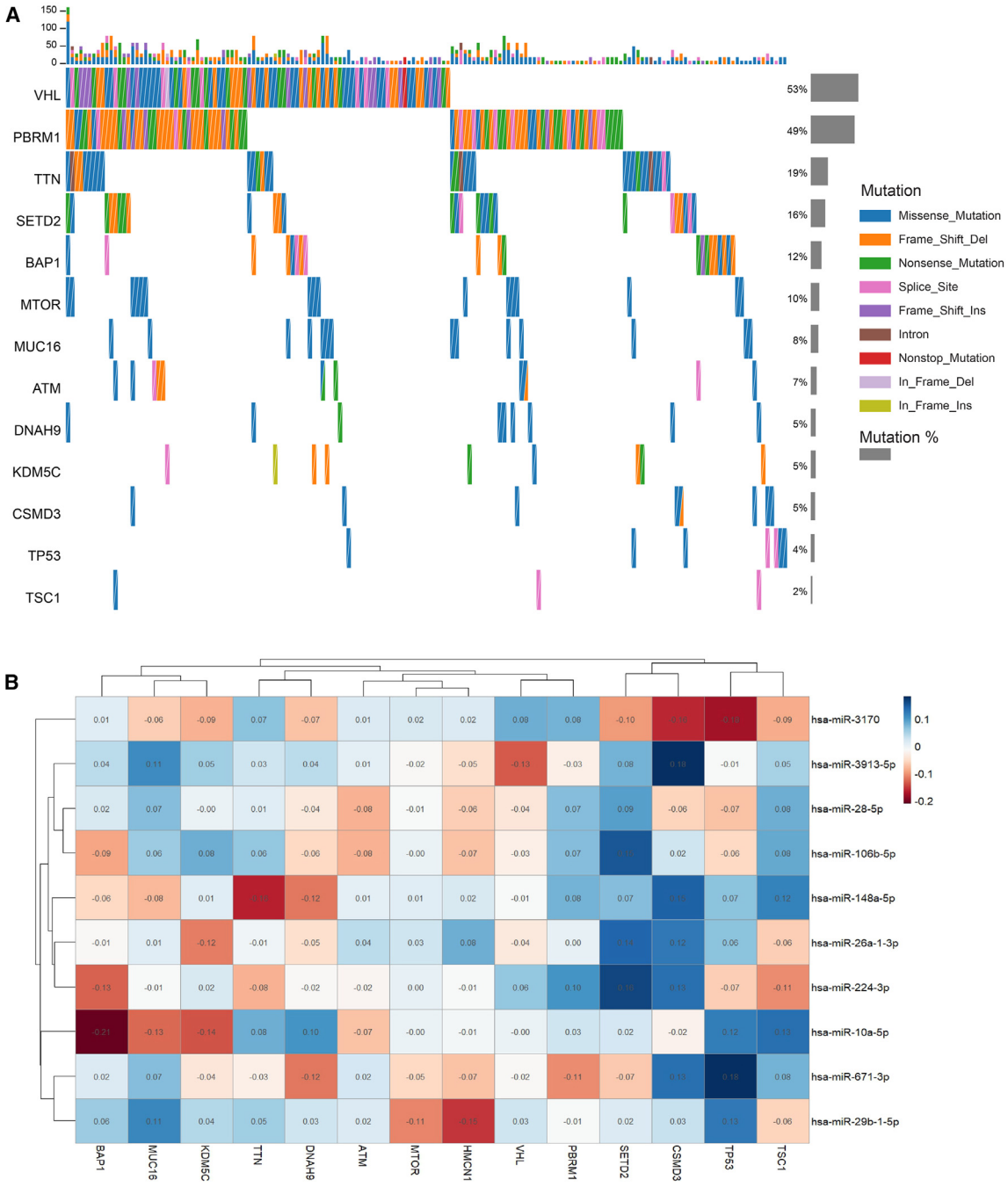

Figure 3. Mutations and miRNA correlation in KIRC

(A) The mutations in KIRC are visualized using Comut-viz. The forest plot highlights the mutated genes and the percentage of KIRC patients with these mutations.

(B) The heatmap illustrates the correlation between the top 10 ranked miRNAs and the mutated genes in KIRC.

The CCs of note in KIRC include P-body (GO:0000932), axon (GO:0030424), clathrin-coated pit (GO:0005905), caveola (GO:0005901), and cytoplasmic stress granule (GO:0010494). Table S11 provides a comprehensive overview of these GO categories for KIRC.

KIRP signature GO annotations

The top BPs for KIRP include miRNA metabolic process (GO:0010586), positive regulation by host of viral transcription (GO:0043923), negative regulation of transcription (GO:0045892),

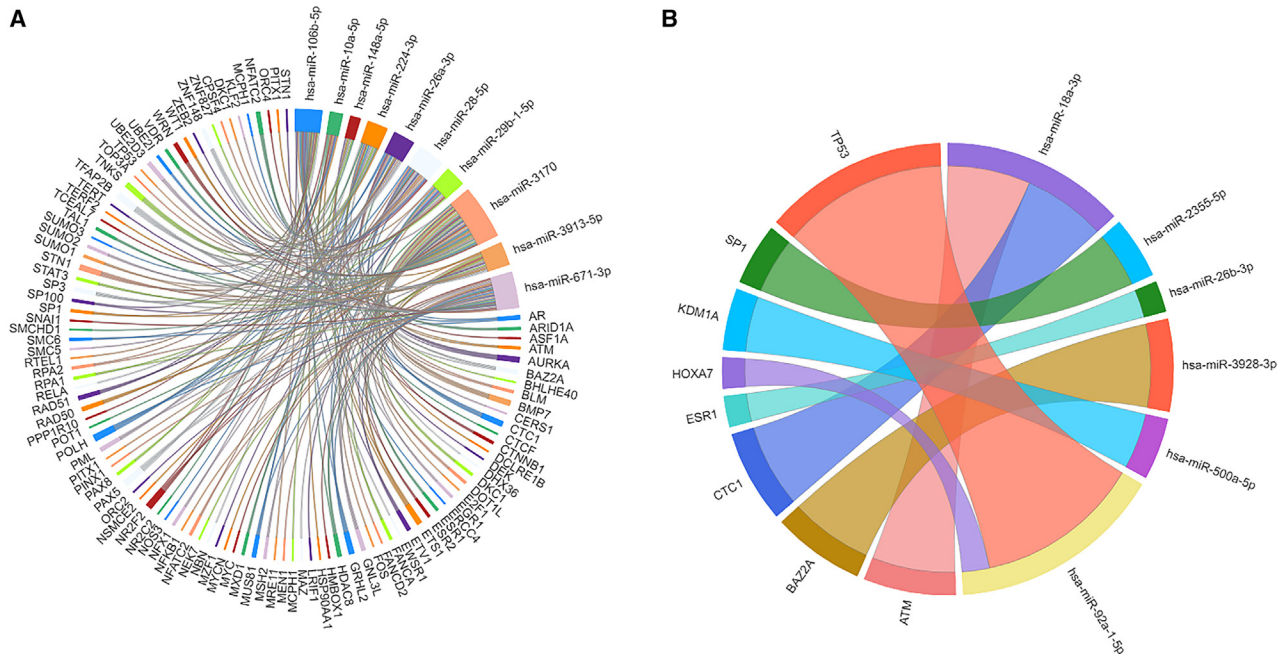

Figure 4. MiRNA-Telomere maintenance gene interaction

(A) Circos plot showing the top KIRC miRNAs targeting 138 TM genes and (B) top KIRP miRNAs targeting eight TM genes.

DNA-templated, production of miRNAs involved in gene silencing by miRNA (GO:0035196), and mRNA splice site selection (GO:0006376).

In KIRP, the leading MFs were DNA-binding transcription activator activity, RNA polymerase II-specific (GO:0001228), transcription regulatory region sequence-specific DNA binding (GO:0000976), DNA-binding transcription factor activity (GO:0003700), transcription factor binding (GO:0008134), and protein serine threonine kinase activity (GO:0004674).

The CCs highlighted in KIRP include RISC complex (GO:0016442), transcription repressor complex (GO:0017053), *cis*-Golgi network (GO:0005801), endoplasmic reticulum-Golgi intermediate compartment membrane (GO:0033116), and cytoplasmic stress granule (GO:0010494). Table S12 details these GO categories for KIRP.

Telomere maintenance in cancer and its association with miRNA signatures

TM is essential for cancer cell proliferation, typically achieved through reactivating telomerase or utilizing the alternative lengthening of telomeres (ALT) pathway. We investigated the relationship between our identified miRNA signatures and TM genes, using the TelNet database to extract validated TM-associated genes.

TM genes and pathway analysis

From the TelNet database, we identified 2,093 human genes linked to TM, including validated, screened, and predicted genes. We focused on 165 validated TM genes with TelNet scores between 4 and 10. KEGG pathway analysis of these TM genes highlighted significant involvement in pathways like mismatch repair (hsa03430), homologous recombination (hsa03440), non-homologous end-joining (hsa03450), Fanconi anemia pathway (hsa03460), cell cycle (hsa04110), cellular senescence (hsa04218), and Th17 cell differentiation (hsa04659). TM genes are also notably active in cancer pathways such as pathways in cancer (hsa05200), prostate cancer (hsa05215), breast cancer (hsa05224), pancreatic cancer (hsa05212), and chronic myeloid leukemia (hsa05220), to name a few. Interestingly, the TM genes (*ATM, TP53, NFKB1, ZEB2, HNRNPK, PDGFRA, MYC, STAT3, UBE2I*, and *E2F1*) were significantly ($p < 0.001$) involved in miRNAs in cancer pathways (hsa05206). More details are in Table S13. GO-BP annotations for TM genes include DNA damage checkpoint (GO:0000077), G1S transition of mitotic cell cycle (GO:0000082), telomere maintenance via recombination (GO:0000722), telomere maintenance via telomerase (GO:0007004), double-strand break repair via homologous recombination (GO:0000724), and DNA double-strand break processing (GO:0000729).

Comparative analysis of miRNA signatures and TM genes

Our comparative analysis of KEGG and GO annotations revealed shared pathways between the KIRC-miRNA signature, KIRP-miRNA signature, and TM genes. The KIRC signature and TM genes share pathways including pancreatic cancer (hsa05212), proteoglycans in cancer (hsa05205), cell cycle (hsa04110), cellular senescence (hsa04218), pathways in cancer (hsa05200), and AGE-RAGE signaling pathway in diabetic complications (hsa04933), detailed in Table 4. Similarly, the KIRP signature and TM genes share pathways

including endocrine resistance (hsa01522), cellular senescence (hsa04218), cell cycle (hsa04110), signaling pathways regulating pluripotency of stem cells (hsa04550), and estrogen signaling pathway (hsa04915), as listed in Table S14. This overlap suggests a significant interplay between miRNA signatures and TM genes in the context of cancer biology.

Common GO annotations in KIRC signature and TM genes

Biological processes

KIRC signature and TM genes shared BPs include angiogenesis (GO:0001525), *in utero* embryonic development (GO:0001701), chromatin remodeling (GO:0006338), cellular response to DNA damage stimulus (GO:0006974), and positive regulation of cell population proliferation (GO:0008284).

Molecular functions

Common MFs were RNA polymerase II transcription regulatory region sequence-specific DNA binding (GO:0000977), protein serine threonine kinase activity (GO:0004674), DNA-binding transcription factor activity (GO:0003700), DNA binding (GO:0003677), and transcription corepressor activity (GO:0003714).

Cellular components

Shared CCs include PML body (GO:0016605), centrosome (GO:0005813), transcription regulator complex (GO:0005667), PML body (GO:0016605), and ribonucleoprotein complex (GO:1990904). Detailed information is in Table S15.

Common GO annotations in KIRP signature and TM genes

Biological processes

Overlapping BPs involve response to hypoxia (GO:0001666), transcription by RNA polymerase II (GO:0006366), cellular response to DNA damage stimulus (GO:0006974), cell cycle (GO:0007049), cell-cycle arrest (GO:0007050), and negative regulation of cell population proliferation (GO:0008285).

Molecular functions

Shared MFs include transcription regulatory region sequence-specific DNA binding (GO:0000976), *cis*-regulatory region sequence-specific DNA binding (GO:0000987), DNA-binding transcription activator activity, RNA polymerase II-specific (GO:0001228), chromatin binding (GO:0003682), and DNA binding (GO:0003677).

Cellular components

Common CCs were transcription regulator complex (GO:0005667), nuclear matrix (GO:0016363), nuclear matrix (GO:0016363), nuclear body (GO:0016604), and ribonucleoprotein complex (GO:1990904). The KIRP signature and TM gene common GO pathways are listed in Table S16.

TM genes in kidney cancer survival predictions

To explore the association of TM genes in kidney cancer survival, we selected the TM genes that are targeted by the identified KIRC and KIRP signatures. Among the 165 validated TM genes, the top 10 miRNAs of the KIRC signature target 100 TM genes. Kaplan-Meier survival analysis revealed that 56 of these genes significantly ($p < 0.05$) correlate with OS in KIRC patients. Among these 100 TM genes, 56 genes significantly ($p \leq 0.05$) predicted the OS in patients with KIRC. Notably, 10 genes, including *BLM, AURKA, AR, PITX1, FANCA, TERT, RTEL1, CTCF, RAD50*, and *MYCN* targeted by specific miRNAs (hsa-miR-26a-1-3p, hsa-miR-28-5p, hsa-miR-3913-5p, hsa-miR-3170, hsa-miR-671-3p, hsa-miR-106b-5p, hsa-miR-26a-1-3p, and hsa-miR-3913-5p), showed a highly significant (<0.0001) association with KIRC patient survival. Detailed information is available in Table S17.

KIRP signature targets seven TM genes, including *CTC1, ATM, SP1, ESR1, BAZ2A, TP53*, and *HOXA7*. These genes were targeted by hsa-miR-18a-3p, hsa-miR-2355-5p, hsa-miR-26b-3p, hsa-miR-376c-3p, hsa-miR-3928-3p, and hsa-miR-92a-1-5p. Among these genes, only one gene *ESR1* showed significant ($p < 0.05$) association with KIRP patient survival (Table S17).

TERT expression levels in KIRC and KIRP

TERT, crucial in cancer development, is hyperactivated in approximately more than 80% of cancers,[30] and its mutations are significantly associated with the survival of KIRC patients.[31] Using UALCAN web tool,[32] we analyzed *TERT* expression in KIRC and KIRP. Our analysis revealed that *TERT* expression was absent in healthy groups, contrasting with the KIRC group. No significant differences in *TERT* levels were noted across various stages, genders, races, and tumor grades in KIRC.

However, a notable difference in *TERT* expression ($p = 0.004$) was found between age groups 41–60 and 81–100 years compared with healthy groups, as shown in Figure S5. *TERT* expression significantly impacts patient survival; Kaplan-Meier survival analysis indicated that higher *TERT* expression correlates with reduced survival in KIRC patients ($p < 0.0001$), as illustrated in Figure S6. Additionally, we assessed the *TERT* promoter methylation profile in KIRC patients vs. healthy individuals. The methylation levels were significantly different between the KIRC and healthy groups ($p < 0.0001$), as indicated in Figure S7, and varied notably between healthy individuals and different KIRC stages, both early and advanced.

A comparison analysis indicated that, similar to KIRC, *TERT* expression was not present in healthy groups but was observed in the KIRP group. Kaplan-Meier survival analysis confirmed that higher *TERT* expression is linked to poorer survival in KIRP patients ($p < 0.0001$), as shown in Figure S8. The methylation levels were significantly different between the KIRP and healthy groups ($p < 0.0001$), with noticeable variations between healthy individuals, detailed in Figure S9.

DISCUSSION

The identification of a miRNA signature predictive of survival in kidney cancer patients could reveal crucial survival biomarkers, enhancing therapeutic strategies. TM genes, known to be involved

Table 4. The shared KEGG pathways between KIRC signature and telomere maintenance genes

KEGG pathways	No. of genes targeted by KIRC signature	*p* values (KIRC)	No. of TM genes	*p* values (TM genes)
Endocrine resistance (hsa01522)	5	0.0059	8	0.0001
Cell cycle (hsa04110)	5	0.0145	11	0.000001
Cellular senescence (hsa04218)	7	0.0028	13	0.000001
Estrogen signaling pathway (hsa04915)	5	0.0215	7	0.003
Thyroid hormone signaling pathway (hsa04919)	5	0.0124	5	0.0223
Relaxin signaling pathway (hsa04926)	6	0.0041	5	0.0298
AGE-RAGE signaling pathway in diabetic complications (hsa04933)	6	0.0012	7	0.0005
Shigellosis (hsa05131)	9	0.002	7	0.0391
Salmonella infection (hsa05132)	7	0.0123	7	0.0254
Hepatitis B (hsa05161)	5	0.0381	12	0.000001
Human cytomegalovirus infection (hsa05163)	6	0.044	11	0.0003
Human papillomavirus infection (hsa05165)	9	0.0147	11	0.0057
Human T cell leukemia virus 1 infection (hsa05166)	8	0.0043	17	0.000001
Kaposi sarcoma-associated herpesvirus infection (hsa05167)	7	0.0061	12	0.000001
Pathways in cancer (hsa05200)	16	0.0007	29	0.000001
Viral carcinogenesis (hsa05203)	8	0.0026	11	0.0001
MicroRNAs in cancer (hsa05206)	12	0.0004	10	0.0099
Colorectal cancer (hsa05210)	5	0.0035	7	0.0002
Pancreatic cancer (hsa05212)	7	<0.0001	7	0.0001
Prostate cancer (hsa05215)	6	0.0011	9	0.000001
Small cell lung cancer (hsa05222)	5	0.0046	6	0.0018
Breast cancer (hsa05224)	5	0.0271	10	0.000001
Hepatocellular carcinoma (hsa05225)	8	0.0009	7	0.0081
Gastric cancer (hsa05226)	5	0.0284	7	0.0044

KIRC, kidney clear cell renal cell carcinoma.

in kidney cancers, show mutations associated with patient survival. While miRNAs regulate telomere function in cancers, their relationship with TM genes in kidney cancer survival remains underexplored. Advancements in understanding the molecular biology of KIRC and KIRP underscore the importance of TM and miRNAs in the progression of these diseases. Telomeres, which protect chromosome ends, are maintained by telomerase and associated proteins.[33] In both KIRC and KIRP, disruption of TM can result in genomic instability and tumor development.[34] MiRNAs can influence the expression of *TERT*, a crucial component of the telomerase complex, affecting telomere length and cellular longevity. Our findings have demonstrated that specific miRNAs, such as hsa-miR-26a-1-3p, hsa-miR-28-5p, and hsa-miR-3913-5p in KIRC, and hsa-miR-450b-5p, hsa-miR-590-5p, and hsa-miR-376c-3p in KIRP, regulate genes linked to telomere biology. Recent research has shown that miR-155 deficiency has been associated with telomeric dysfunction in acute kidney injury.[35] Additionally, changes in miRNA expression profiles are also associated with key genetic mutations in KIRC, such as those in *VHL*, *PBRM1*, and *SETD2*, and in KIRP, highlighting the complex network of genetic and epigenetic factors in these cancers. Exploring these interactions could lead to new targeted therapies that disrupt TM or restore normal miRNA function in KIRC and KIRP patients.

In this study, we developed Evolutionary Learning (EL)-based survival estimation methods KSE-RC and KSE-RP, aiming to identify miRNA signatures predictive of survival in patients with kidney cancers, including KIRC and KIRP. The KSE-RC robust model, featuring 37 miRNAs, achieved an R and MAE of 0.81 and 0.65 years, respectively. For KSE-RP, the highest estimation performance model selected 23 miRNAs as a signature, demonstrating an R and MAE of 0.83 and 0.61 years, respectively, in the comparison of actual and estimated survival times. A notable finding was that hsa-miR-214-5p was the sole miRNA common to both KIRC and KIRP signatures, highlighting each cancer type's distinct miRNA profile. Ranking the miRNA signatures, we identified the top 10 contributing miRNAs

in both KIRC and KIRP, revealing significant expression differences between cancerous and healthy groups. In KIRC, the signature targeted 138 out of 165 validated TM genes, while in KIRP, it targeted eight TM genes.

We discovered shared pathways between miRNA signatures and TM genes. Some common KEGG pathways identified in KIRC and TM genes included proteoglycans in cancer (hsa05205), cell cycle (hsa04110), cellular senescence (hsa04218), pathways in cancer (hsa05200), and AGE-RAGE signaling pathway in diabetic complications. Proteoglycans play a vital role in cell signaling and directly impact carcinogenesis.[36,37] Overexpression of the telomeric repeat-binding factor 2 (*TRF*) has been found to increase levels of glypican-6 and versican, thereby reducing natural killer cell recruitment and cytotoxicity, thereby facilitating tumor progression and metastasis.[38] Lin et al. reported that patients with SPOCK1 proteoglycan tumors had the shortest OS times, indicating a role in KIRC progression.[39] This highlights the complex interplay between proteoglycans and miRNAs in cancer progression.[40] For example, miR-328, found to inhibit a CD44 cell surface proteoglycan, has been shown to play a role in renal tubular cells.[41] Further studies are warranted to explore the regulation of miRNAs and telomere genes in proteoglycan pathways, which could be crucial in understanding kidney cancer survival mechanisms.

Another significant pathway is cellular senescence (hsa04218). Cellular senescence, crucial in embryonic development and wound healing, can become pathological, contributing to aging and various diseases, including chronic kidney disease and acute kidney injury.[42] Telomere length has been linked to renal senescence, renal cysts, and renal RCC,[43] with short telomeres associated with increased renal injury.[44] In our KEGG pathway analysis, the KIRC signature targeted genes such as *PTEN*, *TGFBR2*, *E2F5*, *RBL2*, *MAPK1*, *E2F1*, and *CCND1*, which are significantly involved in cellular senescence. MiRNAs like hsa-miR-125b and hsa-miR-25 in the KIRC signature directly regulate *p53* expression, influencing *p53*-mediated cell-cycle arrest and senescence suppression.[45,46] Additionally, hsa-miR-192 indirectly upregulates *p53* by downregulating the MDM2 oncogene, known to suppress *p53* expression.[46]

Evidence indicates that the top 10 miRNAs of the KIRC signature play critical roles in the disease. Specifically, hsa-miR-26a is dysregulated in KIRC compared with control samples.[47] Hsa-miR-28, which is dysregulated in several malignancies including kidney cancers, is significantly up-regulated in KIRC ($p < 0.05$).[48] An *in vitro* study using RT-qPCR revealed that hsa-miR-671-3p expression is down-regulated in KIRC, impacting the expression of target genes in KIRC.[49] Hsa-miR-224-3p targets glycosylation-related enzymes, activating the PI3K/Akt pathway, which mediates cell proliferation, migration, and invasion in KIRC.[50] Hsa-miR-10a-5p influences tumor immune microenvironment changes and KIRC development by affecting chemokine expression.[51] Dysregulation of hsa-miR-29b in RCC patient CD8+ T cells correlates with dysfunctional immunity in KIRC patients.[52] In KIRP, hsa-miR-590-5p regulates cell proliferation and invasion by targeting *PBRM1*.[53] Hsa-miR-376c-3p is implicated in KIRC,[54] and hsa-miR-18a-3p is associated with kidney diseases.[55] Hsa-miR-362-5p is down-regulated, and hsa-miR-455-5p regulates cell proliferation, migration, and invasion in kidney cancers cancers.[56,57] Decreased expression of hsa-miR-155-5p was identified in chronic kidney disease patients.[58] Collectively, these miRNAs have significant roles in kidney cancers.

In this study, we focused primarily on the exploration of miRNA expression profiles to estimate survival time in patients with KIRC and KIRP. Although the clinical dataset included patients who underwent various treatments such as chemotherapy, immunotherapy, and targeted molecular therapy, the detailed treatment records were available for only 35 out of 512 patients. Additionally, recurrence information was sparse, with 73% of patients lacking recurrence data, 4.5% documented as having a recurrence, and 22.1% documented as having no recurrence. Given these limitations, our analyses emphasized the potential of miRNA expression profiles as robust biomarkers for survival estimation. The results demonstrated that specific miRNAs can reliably predict survival outcomes independent of the treatment regimen. The inclusion of limited therapy and recurrence data did not significantly alter the predictive power of the miRNA profiles, underscoring their strong, independent prognostic value. While our current model does not fully incorporate detailed treatment and recurrence data due to their limited availability, we recognize the importance of these factors. Future studies will aim to integrate comprehensive clinical data to refine and enhance the predictive capabilities of our models further. Despite the limited clinical data, these findings reinforce the importance of miRNA-focused research in improving cancer prognosis and tailoring patient-specific therapeutic strategies.

In summary, our study underscores the potential of miRNA signatures in estimating survival times in KIRC and KIRP. These miRNA signatures may serve as therapeutic targets of TM genes and are involved in significant signaling pathways in kidney cancers. These findings advance future research on miRNA and TM gene interplay in kidney cancer.

MATERIALS AND METHODS

Dataset

The miRNA expression data and clinical characteristics (such as sex, age, tumor stage, and survival time) associated with patients diagnosed with KIRC and KIRP were extracted from The Cancer Genome Atlas (TCGA). There are a total of 512 patients in the KIRC dataset and 283 patients in the KIRP dataset. Following preprocessing steps, which included the removal of duplicate entries and samples lacking survival information, the final datasets comprised 166 samples for KIRC and 168 samples for KIRP. A total of 165 validated genes associated with TM were obtained from the database: http://www.cancertelsys.org/telnet/.

Integration of feature selection and survival estimation methods

The primary objective of this study is to identify a miRNA signature associated with survival and estimate survival times in patients

diagnosed with KIRC and KIRP. To achieve this, we propose an evolutionary learning-based method named KSE, which incorporates an inheritable bi-objective combinatorial genetic algorithm (IBCGA),[59] and support vector regression (SVR).[60] The IBCGA is adept at solving bi-objective combinatorial problems and efficiently selecting a concise set of miRNAs from a pool of 422 candidate miRNAs. In our approach, SVR is employed to estimate survival times based on the actual survival data of patients with kidney cancers. Focusing on the two distinct types of kidney cancers, we developed two models: KSE-RC for KIRC survival and KSE-RP for KIRP survival. The development of the KSE occurs in two steps: one for the KIRC-miRNA signature selection and another for the KIRP-miRNA signature selection. Each miRNA signature selection involves two major components, which include the use of the IBCGA algorithm to select a robust miRNA signature and the estimation of survival time using the identified miRNA signature and SVR. Evaluation of both models in KSE-RC and KSE-RP involved the use of correlation coefficient (R) and mean absolute error (MAE) to assess prediction performance. To ensure robust feature selection in both models, we employed the miRNA frequency (miR*f*) score. The detailed steps in the KSE methodology are as follows.

MiRNA signature selection algorithm

The feature selection algorithm, IBCGA, operates on 422 miRNA expression profiles (n = 422). During the optimization process, the chromosome of IBCGA consists of 422 genes, with three 4-bit genes for encoding γ, C, and ν parameters for the SVR. The detailed steps involved in IBCGA are as follows:

Step 1: Initialization - Randomly generate an initial population of individuals (miRNA profiles).

Step 2: Evaluation - Evaluate the fitness value of all individuals using the fitness function, maximizing the correlation coefficient (R) through 10-fold cross-validation.

Step 3: Selection - Utilize tournament selection to select a winner from two randomly chosen individuals, forming a mating pool.

Step 4: Crossover - Select two parents from the mating pool and perform an orthogonal array crossover operation.

Step 5: Mutation - Apply a conventional mutation operator to randomly selected individuals in the new population.

Step 6: Termination Test - If the stopping condition for obtaining a solution is met, output the best individual as the solution; otherwise, return to Step 2.

Step 7: Inheritance - If r is less than a predefined number of features, randomly change one bit in the binary genetic algorithm-genes for each individual from 0 to 1, increase the number r by one, and return to Step 2. Otherwise, terminate the algorithm.

Estimation of the survival time

Support vector machines (SVMs) have proven effective in cancer diagnosis and prognosis predictions. This study employs SVR to estimate survival time by utilizing miRNA expression profiles and patients' survival data. In our earlier investigations, optimized SVMs played a role in predicting diagnoses for various cancers, including breast cancer[61] and hepatocellular carcinoma,[62,63] as well as prognoses for lung adenocarcinoma, hepatocellular carcinoma, bladder urothelial carcinoma, head and neck carcinoma, and gastrointestinal cancers.[24,64–68] Although the optimization technique is consistent with our prior methods, distinctions lie in the tuning parameters and the selection of robust miRNA signatures.

The SVR optimization problem aims to minimize empirical risk while managing the complexity of the regression function. The basic formulation of the SVR optimization problem is as follows:

Given a dataset $D = \{(x_i, y_i)\}_{i=1}^{N}$ where $x_i \in R^p$ is the input feature vector, and $y_i \in R$ is the corresponding target value, SVR seeks to find a function $f(x)$ subjected to the following optimization problem.

$$\min \left[\left\{ \frac{1}{2} w^T (\varnothing(x_i) + b) + C \left(\nu\varepsilon + \frac{1}{m} \sum_{i=1}^{m} (\xi_i + \xi_i^*) \right) \right\} \right] \quad \text{(Equation 1)}$$

where $0 \leq \nu \leq 1$, $\xi_i \geq 0$, $\xi_i^* \geq 0$, $(x_1, y_1) \ldots (x_m, y_m)$ are the input data points, C is the regularization parameter, ε is an insensitive loss function, and b is a constant.

We conducted 50 independent runs of KSE-RC and KSE-RP. The robust set of miRNA signatures among these 50 independent runs was chosen based on the miRNA frequency (miR*f*) determined through the following procedure:

Step 1: Execute N independent runs of KSE-RC/KSE-RP, maximizing the accuracy of 10-fold cross-validation (10-CV) to obtain N miRNA signatures. Each of these signatures (s), denoted as the r-th signature, comprises Z_r features, where $r = 1 \ldots N$.

Step 2: miR*f* is calculated as follows:

$$miR_f = \sum_{i=1}^{m_t} f(s_i) \Big/ Z_r \quad \text{(Equation 2)}$$

Step 3: Output the f-th feature set with the highest frequency score.

Standard machine learning methods

The performance of KSE was benchmarked against several standard regression methods, encompassing linear regression, SMO regression of Weka,[69] ridge regression,[70] least absolute shrinkage selection operator (LASSO),[71] and elastic net.[72] The minimum λ (lambda) value for ridge, LASSO, and elastic net was determined after 100 iterations of

10-CV. The evaluation of prediction performance was conducted using metrics such as the correlation coefficient (R) and mean absolute error (MAE).

Performance measures

To assess the actual and estimated survival times obtained using KSE, we employed R and mean MAE as the estimation measures to evaluate the prediction performance.

$$R = \frac{\sum_{i=1}^{N}(a_i - \overline{a})(b_i - \overline{b})}{\sqrt{\left[\sum_{i=1}^{N}(a_i - \overline{a})^2\right]\left[\sum_{i=1}^{N}(b_i - \overline{b})^2\right]}} \quad \text{(Equation 3)}$$

where a_i and b_i are the actual and predicted survival times of the ith miRNA, respectively, $\overline{a}$ and $\overline{b}$ are the corresponding means, and N is the total number of KIRC/KIRP patients in the validation set. The MAE is also used for the evaluation of prediction performance, defined as follows:

$$MAE = \frac{1}{N}\sum_{i=1}^{N}|b_i - a_i| \quad \text{(Equation 4)}$$

Clinically significant miRNA by limma association analysis

In this study, we investigated miRNAs associated with tumor stage in both KIRC and KIRP. The tumor stage was categorized into stage I, stage II, stage III, and stage IV for both cancer types. Overall survival (OS), disease-specific survival (DSS), and progression-free interval (PFI) were examined as well. We utilized Limma R package (version 3.50.3) for our analysis. Limma, which stands for "linear models for microarray data," has been widely used for biomarker discovery through the analysis of differential expression in microarray and high-throughput PCR data. It offers functionality for fitting various statistical models, including linear regression and analysis of variance. We normalized the miRNA expression data using log-transformation and adjusted for age at diagnosis and sex. The "makeContrasts" function was then used to perform pairwise comparisons between different stages of cancer in the model.

DATA AND CODE AVAILABILITY

The dataset utilized in this study is available on the TCGA data portal [https://cancergenome.nih.gov/], while genes associated with telomere maintenance can be accessed at http://www.cancertelsys.org/telnet/.

ACKNOWLEDGMENTS

This work was supported in part by institutional funding from Marshfield Clinic Research Institute (MCRI), Marshfield, WI, USA to S.Y.S. and NIGMS grant 1R01GM130715 to S.H. The funders had no role in the study design, data collection and analysis, decision to publish, or preparation of the manuscript.

AUTHOR CONTRIBUTIONS

S.Y.S. designed the system, supervised the study and carried out the detailed study. S.Y.S., S.J., P.S., J.M., R.S., S.-Y.H., and S.H. participated in data analysis, manuscript preparation and discussed the results. All authors have read and approved the final manuscript.

DECLARATION OF INTERESTS

The authors declare no competing interests.

SUPPLEMENTAL INFORMATION

Supplemental information can be found online at https://doi.org/10.1016/j.omton.2024.200874.

REFERENCES

1. American Cancer Society (2023). Cancer Facts & Figures 2023. https://www.cancer.org/content/dam/cancer-org/research/cancer-facts-and-statistics/annual-cancer-facts-and-figures/2023/2023-cancer-facts-and-figures.pdf.
2. Motzer, R.J., Jonasch, E., Agarwal, N., Bhayani, S., Bro, W.P., Chang, S.S., Choueiri, T.K., Costello, B.A., Derweesh, I.H., Fishman, M., et al. (2017). Kidney cancer, version 2. 2017. NCCN clinical practice guidelines in oncology. J. Natl. Compr. Canc. Netw. *15*, 804–834.
3. Znaor, A., Lortet-Tieulent, J., Laversanne, M., Jemal, A., and Bray, F. (2015). International Variations and Trends in Renal Cell Carcinoma Incidence and Mortality. Eur. Urol. *67*, 519–530.
4. Scelo, G., and Larose, T.L. (2018). Epidemiology and risk factors for kidney cancer. J. Clin. Oncol. *36*, 3574–3581.
5. Scelo, G., Li, P., Chanudet, E., and Muller, D.C. (2018). Variability of sex disparities in cancer incidence over 30 years: the striking case of kidney cancer. Eur. Urol. Focus *4*, 586–590.
6. Bukavina, L., Bensalah, K., Bray, F., Carlo, M., Challacombe, B., Karam, J.A., Kassouf, W., Mitchell, T., Montironi, R., O'Brien, T., et al. (2022). Epidemiology of Renal Cell Carcinoma: 2022 Update. Eur. Urol. *82*, 529–542.
7. World Health Organization (2016). The 2016 WHO classification of tumours of the urinary system and male genital organs—part A: renal, penile, and testicular tumours. Eur. Urol. *70*, 93–105.
8. Campbell, S.C., Novick, A.C., Belldegrun, A., Blute, M.L., Chow, G.K., Derweesh, I.H., Faraday, M.M., Kaouk, J.H., Leveillee, R.J., Matin, S.F., et al. (2009). Guideline for management of the clinical T1 renal mass. J. Urol. *182*, 1271–1279.
9. Loo, R.K., Lieberman, S.F., Slezak, J.M., Landa, H.M., Mariani, A.J., Nicolaisen, G., Aspera, A.M., and Jacobsen, S.J. (2013). Stratifying risk of urinary tract malignant tumors in patients with asymptomatic microscopic hematuria. Mayo Clin. Proc. *88*, 129–138.
10. O' Brien, J., Hayder, H., Zayed, Y., and Peng, C. (2018). Overview of MicroRNA Biogenesis, Mechanisms of Actions, and Circulation. Front. Endocrinol. *9*, 402.
11. Garzon, R., Fabbri, M., Cimmino, A., Calin, G.A., and Croce, C.M. (2006). MicroRNA expression and function in cancer. Trends Mol. Med. *12*, 580–587.
12. Sohel, M.M.H. (2020). Circulating microRNAs as biomarkers in cancer diagnosis. Life Sci. *248*, 117473.
13. Sathipati, S.Y., Sharma, R., and Hebbring, S. (2024). Abstract 4892: MicroRNA signature and telomere genes in kidney cancer survival. Cancer Res. *84*, 4892.
14. Gottardo, F., Liu, C.G., Ferracin, M., Calin, G.A., Fassan, M., Bassi, P., Sevignani, C., Byrne, D., Negrini, M., Pagano, F., et al. (2007). Micro-RNA profiling in kidney and bladder cancers. Urol. Oncol. *25*, 387–392. Elsevier.
15. Huang, M., Zhang, T., Yao, Z.-Y., Xing, C., Wu, Q., Liu, Y.-W., and Xing, X.-L. (2021). MicroRNA related prognosis biomarkers from high throughput sequencing data of kidney renal clear cell carcinoma. BMC Med. Genom. *14*, 72.
16. Ng, K.-L., and Taguchi, Y.H. (2020). Identification of miRNA signatures for kidney renal clear cell carcinoma using the tensor-decomposition method. Sci. Rep. *10*, 15149.
17. Bonifacio, L.N., and Jarstfer, M.B. (2010). MiRNA profile associated with replicative senescence, extended cell culture, and ectopic telomerase expression in human foreskin fibroblasts. PLoS One *5*, e12519.
18. Harries, L.W. (2014). MicroRNAs as mediators of the ageing process. Genes *5*, 656–670.
19. Dinami, R., Petti, E., Sestito, R., Benetti, R., and Schoeftner, S. (2014). microRNAs control the function of telomeres in cancer. RNA Disease *1*, ■■■.

20. Pellatt, A.J., Wolff, R.K., Lundgreen, A., Cawthon, R., and Slattery, M.L. (2012). Genetic and lifestyle influence on telomere length and subsequent risk of colon cancer in a case control study. Int. J. Mol. Epidemiol. Genet. *3*, 184–194.

21. Cao, J.-L., Yuan, P., Abuduwufuer, A., Lv, W., Yang, Y.-H., and Hu, J. (2015). Association between the TERT genetic polymorphism rs2853676 and cancer risk: meta-analysis of 76 108 cases and 134 215 controls. PLoS One *10*, e0128829.

22. Pellatt, A.J., Wolff, R.K., Herrick, J., Lundgreen, A., and Slattery, M.L. (2013). TERT's role in colorectal carcinogenesis. Mol. Carcinog. *52*, 507–513.

23. Casuscelli, J., Becerra, M.F., Manley, B.J., Zabor, E.C., Reznik, E., Redzematovic, A., Arcila, M.E., Tennenbaum, D.M., Ghanaat, M., Kashan, M., et al. (2019). Characterization and impact of TERT promoter region mutations on clinical outcome in renal cell carcinoma. Eur. Urol. Focus *5*, 642–649.

24. Yerukala Sathipati, S., and Ho, S.Y. (2017). Identifying the miRNA signature associated with survival time in patients with lung adenocarcinoma using miRNA expression profiles. Sci. Rep. *7*, 7507.

25. Huang, H.-Y., Lin, Y.-C.-D., Cui, S., Huang, Y., Tang, Y., Xu, J., Bao, J., Li, Y., Wen, J., Zuo, H., et al. (2022). miRTarBase update 2022: an informative resource for experimentally validated miRNA–target interactions. Nucleic Acids Res. *50*, D222–D230.

26. Agarwal, V., Bell, G.W., Nam, J.W., and Bartel, D.P. (2015). Predicting effective microRNA target sites in mammalian mRNAs. Elife *4*, e05005.

27. Sticht, C., De La Torre, C., Parveen, A., and Gretz, N. (2018). miRWalk: An online resource for prediction of microRNA binding sites. PLoS One *13*, e0206239.

28. Subramanian, A., Tamayo, P., Mootha, V.K., Mukherjee, S., Ebert, B.L., Gillette, M.A., Paulovich, A., Pomeroy, S.L., Golub, T.R., Lander, E.S., and Mesirov, J.P. (2005). Gene set enrichment analysis: A knowledge-based approach for interpreting genome-wide expression profiles. Proc. Natl. Acad. Sci. USA *102*, 15545–15550.

29. Licursi, V., Conte, F., Fiscon, G., and Paci, P. (2019). MIENTURNET: an interactive web tool for microRNA-target enrichment and network-based analysis. BMC Bioinf. *20*, 545.

30. Shay, J.W., and Wright, W.E. (2005). Senescence and immortalization: role of telomeres and telomerase. Carcinogenesis *26*, 867–874.

31. Hosen, I., Rachakonda, P.S., Heidenreich, B., Sitaram, R.T., Ljungberg, B., Roos, G., Hemminki, K., and Kumar, R. (2015). TERT promoter mutations in clear cell renal cell carcinoma. Int. J. Cancer *136*, 2448–2452.

32. Chandrashekar, D.S., Karthikeyan, S.K., Korla, P.K., Patel, H., Shovon, A.R., Athar, M., Netto, G.J., Qin, Z.S., Kumar, S., Manne, U., et al. (2022). UALCAN: An update to the integrated cancer data analysis platform. Neoplasia *25*, 18–27.

33. Shay, J.W., and Wright, W.E. (2019). Telomeres and telomerase: three decades of progress. Nat. Rev. Genet. *20*, 299–309.

34. Sieverling, L., Hong, C., Koser, S.D., Ginsbach, P., Kleinheinz, K., Hutter, B., Braun, D.M., Cortés-Ciriano, I., Xi, R., Kabbe, R., et al. (2020). Genomic footprints of activated telomere maintenance mechanisms in cancer. Nat. Commun. *11*, 733.

35. Yin, Q., Zhao, Y.J., Ni, W.J., Tang, T.T., Wang, Y., Cao, J.Y., Yin, D., Wen, Y., Li, Z.L., Zhang, Y.L., et al. (2022). MiR-155 deficiency protects renal tubular epithelial cells from telomeric and genomic DNA damage in cisplatin-induced acute kidney injury. Theranostics *12*, 4753–4766.

36. Nikitovic, D., Berdiaki, A., Spyridaki, I., Krasanakis, T., Tsatsakis, A., and Tzanakakis, G.N. (2018). Proteoglycans-Biomarkers and Targets in Cancer Therapy. Front. Endocrinol. *9*, 69.

37. Pinho, S.S., and Reis, C.A. (2015). Glycosylation in cancer: mechanisms and clinical implications. Nat. Rev. Cancer *15*, 540–555.

38. Cherfils-Vicini, J., Iltis, C., Cervera, L., Pisano, S., Croce, O., Sadouni, N., Győrffy, B., Collet, R., Renault, V.M., Rey-Millet, M., et al. (2019). Cancer cells induce immune escape via glycocalyx changes controlled by the telomeric protein TRF2. EMBO J. *38*, e100012.

39. Lin, Y.W., Wen, Y.C., Hsiao, C.H., Lai, F.R., Yang, S.F., Yang, Y.C., Ho, K.H., Hsieh, F.K., Hsiao, M., Lee, W.J., and Chien, M.H. (2023). Proteoglycan SPOCK1 as a Poor Prognostic Marker Promotes Malignant Progression of Clear Cell Renal Cell Carcinoma via Triggering the Snail/Slug-MMP-2 Axis-Mediated Epithelial-to-Mesenchymal Transition. Cells *12*, 352.

40. Piperigkou, Z., Tzaferi, K., Makrokanis, G., Cheli, K., and Karamanos, N.K. (2022). The microRNA-cell surface proteoglycan axis in cancer progression. Am. J. Physiol. Cell Physiol. *322*, C825–C832.

41. Chen, C.H., Cheng, C.Y., Chen, Y.C., Sue, Y.M., Liu, C.T., Cheng, T.H., Hsu, Y.H., and Chen, T.H. (2014). MicroRNA-328 inhibits renal tubular cell epithelial-to-mesenchymal transition by targeting the CD44 in pressure-induced renal fibrosis. PLoS One *9*, e99802.

42. Huang, W., Hickson, L.J., Eirin, A., Kirkland, J.L., and Lerman, L.O. (2022). Cellular senescence: the good, the bad and the unknown. Nat. Rev. Nephrol. *18*, 611–627.

43. Wills, L.P., and Schnellmann, R.G. (2011). Telomeres and telomerase in renal health. J. Am. Soc. Nephrol. *22*, 39–41.

44. Westhoff, J.H., Schildhorn, C., Jacobi, C., Hömme, M., Hartner, A., Braun, H., Kryzer, C., Wang, C., von Zglinicki, T., Kränzlin, B., et al. (2010). Telomere shortening reduces regenerative capacity after acute kidney injury. J. Am. Soc. Nephrol. *21*, 327–336.

45. Munk, R., Panda, A.C., Grammatikakis, I., Gorospe, M., and Abdelmohsen, K. (2017). Chapter Four - Senescence-Associated MicroRNAs. In International Review of Cell and Molecular Biology, *334*, L. Galluzzi and I. Vitale, eds. (Academic Press), pp. 177–205.

46. Suh, N. (2018). MicroRNA controls of cellular senescence. BMB Rep. *51*, 493–499.

47. Chow, T.F.F., Youssef, Y.M., Lianidou, E., Romaschin, A.D., Honey, R.J., Stewart, R., Pace, K.T., and Yousef, G.M. (2010). Differential expression profiling of microRNAs and their potential involvement in renal cell carcinoma pathogenesis. Clin. Biochem. *43*, 150–158.

48. Gottardo, F., Liu, C.G., Ferracin, M., Calin, G.A., Fassan, M., Bassi, P., Sevignani, C., Byrne, D., Negrini, M., Pagano, F., et al. (2007). Micro-RNA profiling in kidney and bladder cancers. Urol. Oncol. *25*, 387–392.

49. Zhu, J., Ma, X., Zhang, Y., Ni, D., Ai, Q., Li, H., and Zhang, X. (2016). Establishment of a miRNA-mRNA regulatory network in metastatic renal cell carcinoma and screening of potential therapeutic targets. Tumour Biol. *37*, 15649–15663.

50. Pan, Y., Hu, J., Ma, J., Qi, X., Zhou, H., Miao, X., Zheng, W., and Jia, L. (2018). MiR-193a-3p and miR-224 mediate renal cell carcinoma progression by targeting alpha-2, 3-sialyltransferase IV and the phosphatidylinositol 3 kinase/Akt pathway. Mol. Carcinog. *57*, 1067–1077.

51. Tan, P., Chen, H., Huang, Z., Huang, M., Du, Y., Li, T., Chen, Z., Liu, Y., and Fu, W. (2021). MMP25-AS1/hsa-miR-10a-5p/SERPINE1 axis as a novel prognostic biomarker associated with immune cell infiltration in KIRC. Mol. Ther. Oncolytics *22*, 307–325.

52. Gigante, M., Pontrelli, P., Herr, W., Gigante, M., D'Avenia, M., Zaza, G., Cavalcanti, E., Accetturo, M., Lucarelli, G., Carrieri, G., et al. (2016). miR-29b and miR-198 overexpression in CD8+ T cells of renal cell carcinoma patients down-modulates JAK3 and MCL-1 leading to immune dysfunction. J. Transl. Med. *14*, 84.

53. Xiao, X., Tang, C., Xiao, S., Fu, C., and Yu, P. (2013). Enhancement of proliferation and invasion by MicroRNA-590-5p via targeting PBRM1 in clear cell renal carcinoma cells. Oncol. Res. *20*, 537–544.

54. Faraonio, R., Salerno, P., Passaro, F., Sedia, C., Iaccio, A., Bellelli, R., Nappi, T.C., Comegna, M., Romano, S., Salvatore, G., et al. (2012). A set of miRNAs participates in the cellular senescence program in human diploid fibroblasts. Cell Death Differ. *19*, 713–721.

55. Aguilar, G., Jiménez, C., Juárez, C., Gómez, R., Rosas, H., and Cruz, D. (2018). 1213 Plasmatic Micrornas Profile Expression in Malignant Pleural Mesothelioma (BMJ Publishing Group Ltd), p. ■■■.

56. Ying, G., Wu, R., Xia, M., Fei, X., He, Q.E., Zha, C., and Wu, F. (2018). Identification of eight key miRNAs associated with renal cell carcinoma: A meta-analysis. Oncol. Lett. *16*, 5847–5855.

57. Yamada, Y., Arai, T., Kojima, S., Sugawara, S., Kato, M., Okato, A., Yamazaki, K., Naya, Y., Ichikawa, T., and Seki, N. (2018). Anti-tumor roles of both strands of the miR-455 duplex: their targets SKA1 and SKA3 are involved in the pathogenesis of renal cell carcinoma. Oncotarget *9*, 26638–26658.

58. Donderski, R., Szczepanek, J., Naruszewicz, N., Naruszewicz, R., Tretyn, A., Skoczylas-Makowska, N., Tyloch, J., Odrowąż-Sypniewska, G., and Manitius, J. (2022). Analysis of profibrogenic microRNAs (miRNAs) expression in urine and

serum of chronic kidney disease (CKD) stage 1–4 patients and their relationship with proteinuria and kidney function. Int. Urol. Nephrol. *54*, 937–947.

59. Ho, S.-Y., Chen, J.-H., and Huang, M.-H. (2004). Inheritable genetic algorithm for biobjective 0/1 combinatorial optimization problems and its applications. IEEE Trans. Syst. Man Cybern. B Cybern. *34*, 609–620.

60. Smola, A.J., and Schölkopf, B. (2004). A tutorial on support vector regression. Stat. Comput. *14*, 199–222.

61. Sathipati, S.Y., Tsai, M.-J., Aimalla, N., Moat, L., Shukla, S.K., Allaire, P., Hebbring, S., Beheshti, A., Sharma, R., and Ho, S.-Y. (2024). An evolutionary learning-based method for identifying a circulating miRNA signature for breast cancer diagnosis prediction. NAR Genom. Bioinform. *6*, lqae022.

62. Yerukala Sathipati, S., and Ho, S.-Y. (2018). Identifying a miRNA signature for predicting the stage of breast cancer. Sci. Rep. *8*, 16138.

63. Yerukala Sathipati, S., and Ho, S.Y. (2020). Novel miRNA signature for predicting the stage of hepatocellular carcinoma. Sci. Rep. *10*, 14452.

64. Yerukala Sathipati, S., Sahu, D., Huang, H.-C., Lin, Y., and Ho, S.-Y. (2019). Identification and characterization of the lncRNA signature associated with overall survival in patients with neuroblastoma. Sci. Rep. *9*, 5125.

65. Yerukala Sathipati, S., Aimalla, N., Tsai, M.-J., Carter, T., Jeong, S., Wen, Z., Shukla, S.K., Sharma, R., and Ho, S.-Y. (2023). Prognostic microRNA signature for estimating survival in patients with hepatocellular carcinoma. Carcinogenesis *44*, 650–661.

66. Yerukala Sathipati, S., Tsai, M.J., Shukla, S.K., Ho, S.Y., Liu, Y., and Beheshti, A. (2022). MicroRNA signature for estimating the survival time in patients with bladder urothelial carcinoma. Sci. Rep. *12*, 4141.

67. Yerukala Sathipati, S., Tsai, M.J., Carter, T., Allaire, P., Shukla, S.K., Beheshti, A., and Ho, S.Y. (2022). Survival estimation in patients with stomach and esophageal carcinoma using miRNA expression profiles. Comput. Struct. Biotechnol. J. *20*, 4490–4500.

68. Yerukala Sathipati, S., and Ho, S.Y. (2023). Survival associated miRNA signature in patients with head and neck carcinomas. Heliyon *9*, e17218.

69. Hall, M., Frank, E., Holmes, G., Pfahringer, B., Reutemann, P., and Witten, I.H. (2009). The WEKA data mining software: an update. SIGKDD Explor. Newsl. *11*, 10–18.

70. Hoerl, A.E., and Kennard, R.W. (1970). Ridge regression: Biased estimation for nonorthogonal problems. Technometrics *12*, 55–67.

71. Tibshirani, R. (1996). Regression shrinkage and selection via the lasso. J. Roy. Stat. Soc. B Stat. Methodol. *58*, 267–288.

72. Zou, H., and Hastie, T. (2005). Regularization and variable selection via the elastic net. J. Roy. Stat. Soc. B Stat. Methodol. *67*, 301–320.